

MADPH-98-1072  
hep-ph/9808299  
August, 1998

## TWO-LOOP EFFECTIVE POTENTIAL CALCULATION OF THE LIGHTTEST $CP$ -EVEN HIGGS-BOSON MASS IN THE MSSM

REN-JIE ZHANG\*

*Department of Physics  
University of Wisconsin  
1150 University Avenue  
Madison, Wisconsin 53706 USA*

### Abstract

We calculate a two-loop effective potential to the order of  $\mathcal{O}(\lambda_t^2 \alpha_s)$  in the MSSM. We then study the corresponding two-loop corrections to the  $CP$ -even Higgs-boson mass for arbitrary  $\tan \beta$  and left-right top-squark mixings. We find that the lightest Higgs-boson mass is changed by at most a few GeV. We also show the improved scale dependence and compare to previous two-loop analyses.

---

\*rjzhang@pheno.physics.wisc.edu

# 1 Introduction

In the minimal supersymmetric standard model (MSSM), the Higgs sector is composed of two neutral  $CP$ -even, one neutral  $CP$ -odd and two charged Higgs bosons. The quartic coupling of the lightest  $CP$ -even Higgs boson is related to the standard model gauge couplings  $g$  and  $g'$  by supersymmetry, as a result, the Higgs boson has a tree-level upper bounded mass  $m_h \leq M_Z$ . However, this limit is invalid when one-loop radiative corrections are included.

The dominant one-loop radiative corrections come from the incomplete cancellation of the virtual top-quark and top-squark loops [1], it approximately has the size  $\Delta m_h^2 \simeq \frac{3\lambda_t^2 m_t^2}{4\pi^2} \log(m_t^2/m_t^2)$ . Taking  $m_{\tilde{t}} = 100 - 1000$  GeV, one finds  $\Delta m_h \simeq$  a few – 50 GeV, due to the relatively large top-quark mass  $m_t^{\text{pole}} = 175$  GeV. The one-loop Higgs-boson mass sensitively depends on the top-quark mass, and generally varies with the renormalization scale. So it remains a quite important problem to study the magnitude of the two-loop radiative corrections and the scale dependence of the Higgs-boson mass once these corrections are considered.

There are basically two approaches to calculate the two-loop radiative corrections. In the renormalization group equation (RGE)-improved effective potential approach [2, 3, 4], one uses the one-loop effective potential, together with two-loop RGEs, then all leading- and next-to-leading-order corrections can be incorporated. The finite one-loop threshold corrections arising from the decouplings of the heavy top-squarks have also been included, both for the small and large left-right top-squark mixings. It is observed that by judiciously setting the renormalization scale, one can use the one-loop renormalized Higgs-boson mass as a good approximation to the full two-loop results [3, 5].

The other approach involves a two-loop effective potential. In the special case of  $\tan \beta \rightarrow \infty$  and no left-right mixing in the top-squark sector, Hempfling and Hoang have calculated the upper bound to the two-loop Higgs-boson mass [6]. Their results qualitatively agree with the previous approach. Recently, two-loop corrections to  $m_h$  have also been computed by an explicit diagrammatic method [7].

It is the purpose of this paper to generalize the two-loop effective potential calculation of [6] to the case of arbitrary  $\tan \beta$  and left-right top-squark mixings. The effective potential method has an advantage over other approaches because it is simple and does not require complicate programming. In this paper we will show the improved scale dependence of the Higgs-boson mass  $m_h$  and the size of two-loop corrections. We will also compare our results with previous two-loop calculations [4, 7].

The paper is organized as follows. In Section 2, we give a general formalism for calculating the  $CP$ -even Higgs-boson mass from the effective potential, and compute the two-loop effective potential to the order of  $\mathcal{O}(\lambda_t^2 \alpha_s)$ . In Section 3, we present the results of our numerical analyses. We find good agreements with previous two-loop calculations. Finally we conclude in Section 4. For completeness, some functions

which appear in the two-loop calculation are given in an Appendix.

## 2 Effective Potential and the $CP$ -even Higgs-boson Masses

We start our analysis with the tree-level potential of the MSSM<sup>†</sup>,

$$\begin{aligned} V_{\text{tree}} = & (m_{H_1}^2 + \mu^2)|H_1|^2 + (m_{H_2}^2 + \mu^2)|H_2|^2 + \mu B(H_1 H_2 + \text{H.c.}) \\ & + \frac{g^2 + g'^2}{8}(|H_1|^2 - |H_2|^2)^2 + \frac{g^2}{2}|H_1^\dagger H_2|^2, \end{aligned} \quad (1)$$

where  $g, g'$  are the  $SU(2)$  and  $U(1)_Y$  gauge couplings,  $m_{H_1}, m_{H_2}$  and  $B$  are the soft-breaking Higgs-sector mass parameters, and  $\mu$  is the supersymmetric Higgs-boson mass parameter.

We express the fields  $H_1$  and  $H_2$  in terms of their component fields,

$$H_1 = \begin{pmatrix} (S_1 + iP_1)/\sqrt{2} \\ H_1^- \end{pmatrix}, \quad H_2 = \begin{pmatrix} H_2^+ \\ (S_2 + iP_2)/\sqrt{2} \end{pmatrix}, \quad (2)$$

so the tree-level potential can be rewritten as a function of the  $CP$ -even fields  $S_1$  and  $S_2$ . The effective potential is then a function of  $S_1$  and  $S_2$ , which are usually known as classical fields. The condition of the electro-weak symmetry breaking is imposed by minimizing the effective potential with respect to the classical fields.

The technique for calculating a higher loop effective potential was developed long ago by Jackiw [9]. The Higgs fields are expanded around the classical fields, and all the relevant particle masses and couplings are determined as functions of the classical fields. One then calculates the higher loop effective potential by computing the corresponding Feynman diagrams.

To be more specific, to the two-loop order that we consider in this paper, we write the effective potential as

$$V(S_1, S_2) = V_0 + V_{\text{tree}}(S_1, S_2) + V_{\text{1loop}}(S_1, S_2) + V_{\text{2loop}}(S_1, S_2), \quad (3)$$

where  $V_0$  is a field-independent vacuum-energy, and  $V_{\text{tree}}$ ,  $V_{\text{1loop}}$  and  $V_{\text{2loop}}$  are the tree-, one- and two-loop contributions respectively.  $V_0$  is necessary for the renormalization group invariance of the effective potential [10].

The one-loop effective potential in the  $\overline{\text{DR}}$  scheme is well-known. It can be easily obtained by calculating the one-loop bubble diagrams with all kinds of (s)particles running in the loop. We find that in the Landau gauge

$$V_{\text{1loop}}(S_1, S_2) = \sum_f \sum_{i=1}^2 N_c^f G(\tilde{f}_i) - 2 \sum_f N_c^f G(f) + 3G(W) + \frac{3}{2}G(Z)$$

---

<sup>†</sup>We work in the modified  $\overline{\text{DR}}$  -scheme of Ref. [8].

$$\begin{aligned}
&+ \frac{1}{2} \left[ G(H) + G(h) + G(A) + G(G) \right] + G(H^+) + G(G^+) \\
&- 2 \sum_{i=1}^2 G(\tilde{\chi}_i^+) - \sum_{i=1}^4 G(\tilde{\chi}_i^0) ,
\end{aligned} \tag{4}$$

where  $f$  sums over all the (s)quarks and (s)leptons,  $N_c^f$  is the color factor, 3 for (s)quarks and 1 for (s)leptons, and all the masses are implicitly  $S_1$ ,  $S_2$ -dependent. We have used short-handed notations  $\tilde{f}_i = m_{\tilde{f}_i}^2$  etc. The function  $G(x)$  is defined by

$$G(x) = \frac{x^2}{32\pi^2} \left( \overline{\ln} x - \frac{3}{2} \right), \tag{5}$$

where  $\overline{\ln} x = \ln(x/Q^2)$  and  $Q$  is the renormalization scale.

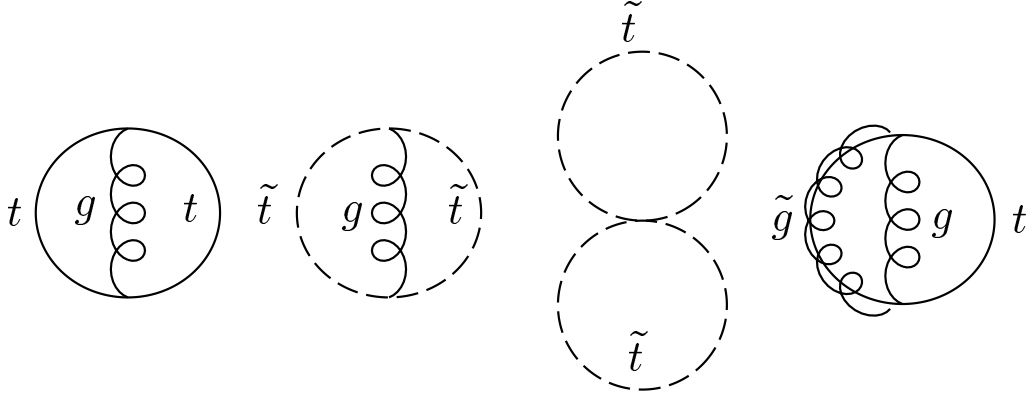


Figure 1: Bubble diagrams for the two-loop effective potential to the order of  $\mathcal{O}(\lambda_t^2 \alpha_s)$  in the MSSM.

The two-loop effective potential can be derived similarly, the corresponding Feynman diagrams are depicted in Fig. 1. To the order of  $\mathcal{O}(\lambda_t^2 \alpha_s)$ , we have in the Landau gauge

$$\begin{aligned}
V_{\text{2loop}}(S_1, S_2) = & 32\pi\alpha_s \left\{ J(t, t) - 2t I(t, t, 0) \right. \\
& + \frac{1}{2} (c_t^4 + s_t^4) \sum_{i=1}^2 J(\tilde{t}_i, \tilde{t}_i) + 2s_t^2 c_t^2 J(\tilde{t}_1, \tilde{t}_2) + \sum_{i=1}^2 \tilde{t}_i I(\tilde{t}_i, \tilde{t}_i, 0) \\
& \left. + \sum_{i=1}^2 L(\tilde{t}_i, \tilde{g}, t) - 4\tilde{g} t s_t c_t \left( I(\tilde{t}_1, \tilde{g}, t) - I(\tilde{t}_2, \tilde{g}, t) \right) \right\} \tag{6}
\end{aligned}$$

where the (minimally) subtracted functions  $I$  and  $J$  are defined in the Appendix,  $s_t$  is the top-squark mixing angle. A two-loop effective potential at the  $\tan\beta \rightarrow \infty$  and no left-right squark-mixing limit  $s_t = 0$  has been obtained in Ref. [6]. As a good check, one can show that the effective potential  $V(S_1, S_2)$  is invariant under

the renormalization scale change, up to two-loop terms which are ignored in our approximation.

The effective potential Eq. (6), as a generating functional, encodes all the two-loop information. From this we can obtain two-loop tadpoles and self-energies at zero external momenta, and subsequently the two-loop  $CP$ -even Higgs-boson masses by solving appropriate on-mass-shell conditions.

We first minimize  $V(S_1, S_2)$  at the Higgs vacuum expectation values  $S_1 = v_1$  and  $S_2 = v_2$ ,

$$\frac{\partial V}{\partial S_1} \Big|_{S_1=v_1, S_2=v_2} = 0, \quad \frac{\partial V}{\partial S_2} \Big|_{S_1=v_1, S_2=v_2} = 0. \quad (7)$$

This is equivalent to the requirement that the tadpoles vanish,

$$\frac{T_1}{v_1} = \frac{1}{2} m_Z^2 c_{2\beta} + m_{H_1}^2 + \mu^2 + B\mu \tan \beta, \quad (8)$$

$$\frac{T_2}{v_2} = -\frac{1}{2} m_Z^2 c_{2\beta} + m_{H_2}^2 + \mu^2 + B\mu \cot \beta, \quad (9)$$

where  $\tan \beta = v_2/v_1$ ,  $m_Z^2 = (g^2 + g'^2)v^2/4$  and  $v^2 = v_1^2 + v_2^2$ . To the two-loop order, the tadpoles  $T_i$ ,  $i = 1, 2$  are given by  $T_i = T_i^{1\text{loop}} + T_i^{2\text{loop}}$ , where the one- and two-loop tadpoles are defined by

$$T_i^{1\text{loop}} = -\left(\frac{\partial V_{1\text{loop}}}{\partial S_i}\right) \Big|_{S_1=v_1, S_2=v_2}, \quad T_i^{2\text{loop}} = -\left(\frac{\partial V_{2\text{loop}}}{\partial S_i}\right) \Big|_{S_1=v_1, S_2=v_2}. \quad (10)$$

One can check that the one-loop tadpoles  $T_i^{1\text{loop}}$  deduced in this way give the same results as in Ref. [11]<sup>‡</sup>, where they were obtained by explicitly calculating the tadpole diagrams.

The  $CP$ -even Higgs-boson mass matrix, after some algebra, is

$$\begin{aligned} \mathcal{M}^2(p^2) = & \\ \begin{pmatrix} m_Z^2 c_\beta^2 + m_A^2 s_\beta^2 - \text{Re}\Pi_{11}(p^2) + T_1/v_1 & -(m_Z^2 + m_A^2) s_\beta c_\beta - \text{Re}\Pi_{12}(p^2) \\ -(m_Z^2 + m_A^2) s_\beta c_\beta - \text{Re}\Pi_{12}(p^2) & m_Z^2 s_\beta^2 + m_A^2 c_\beta^2 - \text{Re}\Pi_{22}(p^2) + T_2/v_2 \end{pmatrix}, \end{aligned} \quad (11)$$

where  $m_A^2 = -\mu B(\tan \beta + \cot \beta)$ , and both  $m_Z$  and  $m_A$  are  $\overline{\text{DR}}$  running masses.

Finally, the radiatively corrected Higgs-boson masses can be found by computing the zeroes of the inverse propagator,  $p^2 - \mathcal{M}^2(p^2)$ . To keep all one-loop contributions, we use the complete formulae for the one-loop self-energies  $\Pi_{ij}^{1\text{loop}}(p^2)$  and tadpoles  $T_i^{1\text{loop}}/v_i$  given at Ref. [11]. The two-loop self-energies at the zero external momentum are found from the two-loop effective potential (6) by

$$\Pi_{ij}^{2\text{loop}}(0) = -\left(\frac{\partial^2 V_{2\text{loop}}}{\partial S_i \partial S_j}\right) \Big|_{S_1=v_1, S_2=v_2}, \quad i, j = 1, 2. \quad (12)$$

---

<sup>‡</sup>In Ref. [11], we used the 't Hooft-Feynman gauge. To compare with the one-loop tadpoles obtained from Eq. (4), the Goldstone boson masses need to be set to zero.

### 3 Numerical Procedure and Results

We first show the improvement of the renormalization scale ( $Q$ ) dependence of the lightest  $CP$ -even Higgs-boson mass. The procedure for this part of numerical analysis proceeds as follows: We solve two-loop renormalization group equations (RGEs) of the MSSM subjected to two-sided boundary conditions. At the electro-weak scale  $M_Z$ , we take the observables  $\alpha_s$ ,  $\alpha_{em}$ ,  $G_F$ ,  $M_Z$ ,  $m_t$ ,  $m_b$  and  $m_\tau$  from the experiment as inputs, and at the unification scale  $M_{\text{GUT}} \approx 2 \times 10^{16}$  GeV, we assume the universality and take a common scalar mass  $M_0$ , a common gaugino mass  $M_{1/2}$  and a trilinear scalar coupling  $A_0$  as inputs. (This is sometimes called the minimal supergravity (mSUGRA) model.) Low energy threshold corrections to the gauge and Yukawa couplings have been properly taken into account as in Ref. [11].

The  $\mu$ -parameter and the (tree-level) mass  $m_A$  are determined in terms of other variables through the minimization conditions (8) and (9) which ensure the right electro-weak symmetry breaking,

$$\mu^2 = \frac{1}{2} \left[ \tan 2\beta \left( \overline{m}_{H_2}^2 \tan \beta - \overline{m}_{H_1}^2 \cot \beta \right) - m_Z^2 \right], \quad (13)$$

$$m_A^2 = \frac{1}{\cos 2\beta} \left( \overline{m}_{H_2}^2 - \overline{m}_{H_1}^2 \right) - m_Z^2, \quad (14)$$

where  $\overline{m}_{H_1}^2 = m_{H_1}^2 - T_1/v_1$  and  $\overline{m}_{H_2}^2 = m_{H_2}^2 - T_2/v_2$ .

We then calculate the lightest  $CP$ -even Higgs-boson mass from the mass matrix Eq. (12). We use the one-loop tadpole and self-energy formulae from Ref. [11], while for the two-loop contributions, we compute the tadpoles and self-energies numerically according to Eqs. (10) and (12) by replacing the differentiation by a finite difference. The field-dependent masses in Eq. (6) are the top-quark mass  $m_t = \lambda_t S_2/\sqrt{2}$  and the top-squark masses which are found from the following field-dependent mass matrix:

$$\begin{pmatrix} M_Q^2 + \frac{1}{2}\lambda_t^2 S_2^2 & \frac{1}{\sqrt{2}}\lambda_t(A_t S_2 + \mu S_1) \\ \frac{1}{\sqrt{2}}\lambda_t(A_t S_2 + \mu S_1) & M_U^2 + \frac{1}{2}\lambda_t^2 S_2^2 \end{pmatrix}, \quad (15)$$

where we have neglected the field-dependent  $D$ -term contributions and  $M_Q, M_U$  are soft squark masses at the low-energy scale. The field-dependent angle  $s_t$  in Eq. (6) is defined as the mixing angle of the above mass matrix.

In Fig. 2, we show the dependence of the one- and two-loop radiatively corrected  $CP$ -even Higgs-boson masses  $m_h$  on the renormalization scale  $Q$ . We choose the universal parameters  $M_0 = 500$  GeV,  $M_{1/2} = 200$  GeV and  $A_0 = 0$  at the unification scale, the sign of  $\mu$ -parameter is set to be negative<sup>§</sup>. We plot two choices of  $\tan \beta = 2$  and 20. The one- and two-loop masses are shown in dashed and solid lines. For the corrections to the Higgs-boson masses  $m_h$ , we have used the  $\overline{\text{DR}}$  running top-Yukawa

---

<sup>§</sup>Our convention of the sign of  $\mu$ -parameter is opposite to that of Refs. [4] and [7].

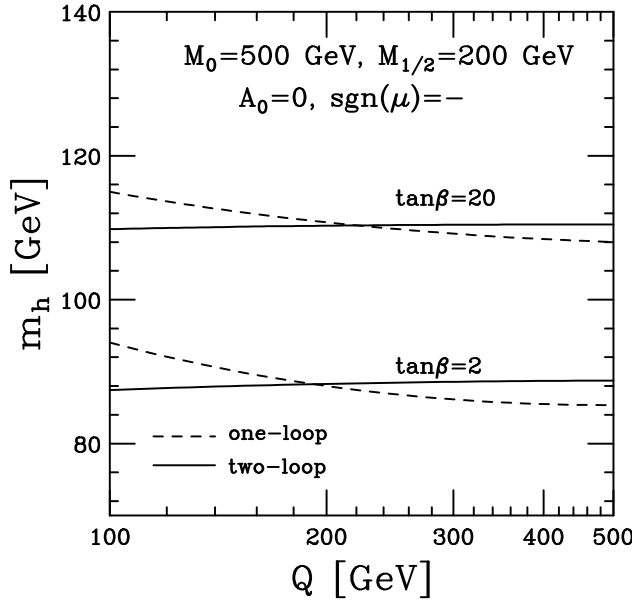


Figure 2: The renormalization-scale ( $Q$ ) dependence of the lightest  $CP$ -even Higgs-boson mass  $m_h$ . The dashed and solid lines correspond to the one- and two-loop masses respectively. We have fixed the universal boundary conditions  $M_0 = 500$  GeV,  $M_{1/2} = 200$  GeV and  $A_0 = 0$ , the sign of  $\mu$ -parameter is chosen to be negative.

coupling  $\lambda_t$  at the scale  $Q$ . The formulae which convert the top-quark pole mass  $m_t^{\text{pole}}$  to  $\lambda_t(Q)$  are given in Ref. [11].

We see that the one-loop radiatively corrected Higgs-boson masses vary by about 10 GeV as the renormalization scale  $Q$  varies from 100 to 500 GeV. However, once we properly include the two-loop radiative corrections, the scale dependence of  $m_h$  becomes much milder, and we find  $m_h = 88$  GeV and 110 GeV for  $\tan\beta = 2$  and 20 to a good precision for all ranges of the scale. The two-loop calculation can only change  $m_h$  by a few GeV.

In Figs. 3 and 4, we compare our results with that of RGE-improved effective potential (EP) approach [4]. In that approach, the heavy particles are decoupled at  $m_{\tilde{t}}$  or  $m_{\tilde{t}_1}$  and  $m_{\tilde{t}_2}$  stepwisely if they are very different. The two-loop RGEs of the effective field theory below the decoupling scale is then used to run the effective couplings to the scale where the Higgs-boson mass is evaluated, *e.g.* the on-shell top-quark mass. Since the next-to-leading-order corrections are negligible at this scale [3], it allows an analytical solution to the two-loop RGEs [4].

For this part of numerical analysis, we do not impose the minimization conditions Eqs. (8) and (9), and the  $\mu$ -parameter and the  $CP$ -odd Higgs boson mass  $m_A$  are treated as inputs. The soft squark masses are taken as  $M_Q = M_U = M_S$ . In Fig. (3), we show the two-loop Higgs-boson masses  $m_h$  versus the soft squark mass  $M_S$  in the RGE-improved one-loop EP approach (dashed lines) and the two-loop EP approach

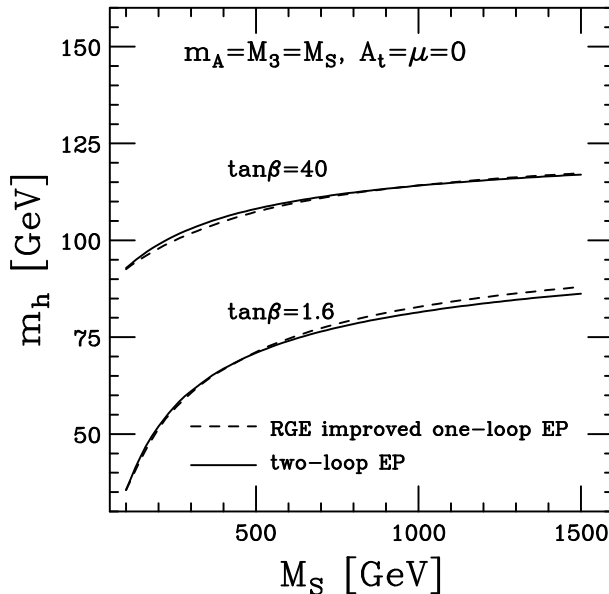


Figure 3: Higgs boson masses  $m_h$  vs. the squark soft masses  $M_S$  in the no-squark-mixing case  $A_t = \mu = 0$ . The solid lines are results from the two-loop EP approach. For comparison, we also show the results from the RGE-improved one-loop EP approach in dashed lines.

(solid lines). The parameters  $A_t$  and  $\mu$  are set to zero, which corresponds to the no left-right squark-mixing limit. Other parameters are  $m_A = M_3 = M_S$ . We see a remarkable agreement of the results from the two approaches, for both small and large  $\tan \beta$  cases.

In Fig. (4), we choose nonzero  $\mu$ -parameter  $\mu = -200$  GeV and plot  $m_h$  versus  $X_t/M_S$  where  $X_t = A_t + \mu/\tan \beta$  is related to the off-diagonal element of the squark-mass matrix. We see the results from the two approaches still agree quite well except for the large positive  $X_t/M_S$ . In particular, the curves for the two-loop EP approach peak at  $X_t/M_S = 2$ , which is different from the RGE-improved one-loop EP approach. This however agrees with the results of a recent analysis [7]. We found that for  $\tan \beta = 40$  the upper limit for the Higgs-boson mass is 125 GeV at the large squark-mixing ( $X_t/M_S = \pm 2$ ).

## 4 Conclusions

To conclude, we have used an effective potential method to calculate the two-loop corrections to the lightest  $CP$ -even Higgs-boson mass in the MSSM. Our approach is straightforward and easy to program, and can be extended to include two-loop corrections of order  $\mathcal{O}(\lambda_t^4)$ . We show that the renormalization scale dependence of  $m_h$  improves after including the two-loop corrections, this largely reduces the

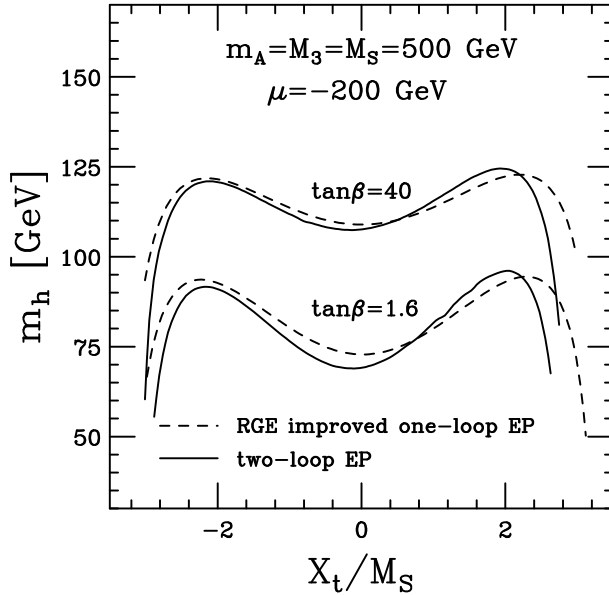


Figure 4: Higgs-boson masses  $m_h$  vs.  $X_t/M_S$ , where  $X_t = A_t + \mu/\tan\beta$ . Both the results from the RGE-improved one-loop EP and two-loop EP approaches are shown.

uncertainty associated with one-loop calculations. We have shown that the two-loop correction is only about a few GeV with respect to the one-loop results (where the  $\overline{\text{DR}}$  running coupling  $\lambda_t$  is used). We have also compared our results with some previous two-loop calculations. We found good agreements with the RGE-improved one-loop EP approach of Ref. [4] except for the case of large left-right squark mixing, where we obtained similar results as in Ref. [7]. The upper bound for the Higgs-boson mass  $m_h \lesssim 125$  GeV is achieved at the region of parameter space for large  $\tan\beta$  and left-right squark mixings.

## Acknowledgements

I would like to thank K. Matchev for participating in the early stage of this work, J. Bagger, C. Kao and T. Han for conversations and comments, and C. Wagner and G. Weiglein for communications and numerical comparisons. This work was supported in part by a DOE grant No. DE-FG02-95ER40896 and in part by the Wisconsin Alumni Research Foundation.

## Appendix: The functions $I(x, y, z)$ and $J(x, y)$

Momentum integrals arising from the two-loop bubble diagrams have one-loop

subdivergences which can be subtracted in the standard way [12]. Furthermore, in the  $\overline{\text{DR}}$  scheme there is no complication associated with vector-boson loops<sup>¶</sup>, so all integrals can be expressed in terms of (minimally) subtracted functions  $I$ ,  $J$  which are [12]

$$(16\pi^2)^2 J(x, y) = x y \left[ 1 - \overline{\ln} x - \overline{\ln} y + \overline{\ln} x \overline{\ln} y \right], \quad (\text{A.1})$$

$$\begin{aligned} (16\pi^2)^2 I(x, y, z) = & -\frac{1}{2} \left[ (y + z - x) \overline{\ln} y \overline{\ln} z + (z + x - y) \overline{\ln} z \overline{\ln} x \right. \\ & \left. + (x + y - z) \overline{\ln} x \overline{\ln} y - 4(x \overline{\ln} x + y \overline{\ln} y + z \overline{\ln} z) + \xi(x, y, z) + 5(x + y + z) \right], \end{aligned} \quad (\text{A.2})$$

where  $\xi$  is given by

$$\xi(x, y, z) = 8b \left[ L(\theta_x) + L(\theta_y) + L(\theta_z) - \frac{\pi}{2} \ln 2 \right] \quad (\text{A.3})$$

when  $-b^2 = a^2 = (x^2 + y^2 + z^2 - 2xy - 2xz - 2yz)/4 \leq 0$ , and

$$\xi(x, y, z) = 8a \left[ -M(-\phi_x) + M(\phi_y) + M(\phi_z) \right] \quad (\text{A.4})$$

when  $a^2 > 0$ . Here  $L(t)$  is Lobachevsky's function, defined as

$$L(t) = - \int_0^t dx \ln \cos x = t \ln 2 - \frac{1}{2} \sum_{k=1}^{\infty} (-)^{k-1} \frac{\sin 2kt}{k^2}, \quad (\text{A.5})$$

and the function  $M(t)$  is defined as

$$M(t) = - \int_0^t dx \ln \sinh x = \frac{\pi^2}{12} - \frac{t^2}{2} + t \ln 2 - \frac{1}{2} \text{Li}_2(e^{-2t}), \quad (\text{A.6})$$

$\text{Li}_2$  is the dilogarithm function.

The angles  $\theta_{x,y,z}$  and  $\phi_{x,y,z}$  are defined by

$$\theta_x = \arctan \left( \frac{y + z - x}{2b} \right), \quad \phi_x = \operatorname{arccoth} \left( \frac{y + z - x}{2a} \right), \quad \text{etc.} \quad (\text{A.7})$$

Finally we have also used the following function in the two-loop effective potential:

$$L(x, y, z) = J(y, z) - J(x, y) - J(x, z) - (x - y - z) I(x, y, z). \quad (\text{A.8})$$

---

<sup>¶</sup>In contrast, the vector bosons live in  $d = 4 - 2\epsilon$  dimensions in the  $\overline{\text{MS}}$  scheme, in reducing the two-loop integrals to the form of  $I$  and  $J$ , there will be extra finite terms from themselves and the associated one-loop subdiagrams.

## References

- [1] S.P. Li and M. Sher, Phys. Lett. **B140** (1984) 339; Y. Okada, M. Yamaguchi, and T. Yanagida, Prog. Theor. Phys. **85** (1991) 1; Phys. Lett. **B262** (1991) 54; J. Ellis, G. Ridolfi and F. Zwirner, Phys. Lett. **B257** (1991) 83; H.E. Haber and R. Hempfling, Phys. Rev. Lett. **66** (1991) 1815; R. Barbieri, M. Frigeni and M. Caravaglios, Phys. Lett. **B263** (1991) 233; P.H. Chankowski, preprint IFT-7-91-WARSAW (1991); J.R. Espinosa and M. Quiros, Phys. Lett. **B266** (1991) 389; J.L. Lopez and D.V. Nanopoulos, Phys. Lett. **B266** (1991) 397; D.M. Pierce, A. Papadopoulos and S.B. Johnson, Phys. Rev. Lett. **68** (1992) 3678; A. Brignole, Phys. Lett. **B281** (1992) 284; P.H. Chankowski, S. Pokorski and J. Rosiek, Nucl. Phys. **B423** (1994) 437; A. Dabelstein, Z. Phys. **C67** (1995) 495.
- [2] J. Kodaira, Y. Yasui and K. Sasaki, Phys. Rev. **D50** (1994) 7035; A.V. Gladyshev and D.I. Kazakov, Mod. Phys. Lett. **A10** (1995) 3129; M. Carena, J.R. Espinosa, M. Quiros and C.E.M. Wagner, Phys. Lett. **B355** (1995) 209.
- [3] J.A. Casas, J.R. Espinosa, M. Quiros and A. Riotto, Phys. Lett. **B436** (1995) 3.
- [4] M. Carena, M. Quiros and C.E.M. Wagner, Nucl. Phys. **B461** (1996) 407.
- [5] H.E. Haber, in *Brussels EPS HEP 1995*, [hep-ph/9601330](#); H.E. Haber, R. Hempfling and A. Hoang, Z. Phys. **C75** (1997) 539.
- [6] R. Hempfling and A.H. Hoang, Phys. Lett. **B331** (1994) 99.
- [7] S. Heinemeyer, W. Hollik and G. Weiglein, [hep-ph/9803277](#); [hep-ph/9807423](#).
- [8] I. Jack, D.R.T. Jones, S.P. Martin, M.T. Vaughn and Y. Yamada, Phys. Rev. **D50** (1994) 5481.  
The original  $\overline{\text{DR}}$  scheme was discussed in  
W. Siegel, Phys. Lett. **B84** (1979) 193; D.M. Capper, D.R.T. Jones and P. van Nieuwenhuizen, Nucl. Phys. **B167** (1980) 479.
- [9] R. Jackiw, Phys. Rev. **D9** (1974) 1686.
- [10] B. Kastening, Phys. Lett. **B283** (1992) 287.
- [11] D.M. Pierce, J.A. Bagger, K.T. Matchev and R.-J. Zhang, Nucl. Phys. **B491** (1997) 3.
- [12] C. Ford and D.R.T. Jones, Phys. Lett. **B274** (1992) 409; C. Ford, I. Jack and D.R.T. Jones, Nucl. Phys. **B387** (1992) 373.